Comparative analysis of numerical and experimental data of orthodontic mini-implants

Athina Chatzigianni*, Ludger Keilig*, Heinz Duschner**, Hermann Götz**, Theodore Eliades*** and Christoph Bourauel*

*Oral Technology, University of Bonn, Germany, **Applied Structure and Microanalysis, Johannes Gutenberg-University, Mainz, Germany and ***Department of Orthodontics, Aristotle University of Thessaloniki, Greece

Correspondence to: Theodore Eliades, 57 Agnoston Hiroon, Nea Ionia 14231, Greece. E-mail: teliades@ath.forthnet.gr

SUMMARY The purpose of this study was to compare numerical simulation data derived from finite element analysis (FEA) to experimental data on mini-implant loading. Nine finite element (FE) models of mini-implants and surrounding bone were derived from corresponding experimental specimens. The animal bone in the experiment consisted of bovine rib. The experimental groups were based on implant type, length, diameter, and angle of insertion. One experimental specimen was randomly selected from each group and was digitized in a microCT scanner. The FE models consisted of bone pieces containing Aarhus mini-implants with dimensions 1.5 × 7 mm and 1.5 × 9 mm or LOMAS mini-implants (dimensions 1.5 × 7 mm, 1.5 × 9 mm, and 2 × 7 mm). Mini-implants were inserted in two different ways, perpendicular to the bone surface or at 45 degrees to the direction of the applied load. Loading and boundary conditions in the FE models were adjusted to match the experimental situation, with the force applied on the neck of the mini-implants, along the mesio-distal direction up to a maximum of 0.5 N. Displacement and rotation of mini-implants after force application calculated by FEA were compared to previously recorded experimental deflections of the same mini-implants. Analysis of data with the Altman–Bland test and the Youden plot demonstrated good agreement between numerical and experimental findings (P = not significant) for the models selected. This study provides further evidence of the appropriateness of the FEA as an investigational tool in relevant research.

Introduction

The finite element analysis (FEA) or finite element method (FEM), a numerical method from engineering sciences, used to obtain approximate numerical solutions to the abstract equations of calculus that predict the response of physical systems, which are subjected to external influences (Knox *et al.*, 2000), has been extensively utilized in contemporary dental research. In the FEA, the body to be analysed consists of a large number of small elements building a mesh that is sufficient to describe the geometry of the subject. Elements consist of element edges and faces, which are connected by points called nodes. The nodes are characterized by their global co-ordinates and symbolized by a spot on the screen. According to the number of nodes, the shape of an element can be a line, triangle, square, or a mixed element. Depending on the complexity of the examined structure and the desired analysis, the finite element (FE) model generation and its numerical calculation can vary from quite simple to very complex and highly sophisticated.

The FEA was introduced to dental biomedical research in 1973 (Farah *et al.*, 1973) and since then has been extensively applied to analyse the stress and strain in the alveolar supporting structures and especially in the periodontal ligament (PDL; Kawarizadeh *et al.*, 2003; Natali *et al.*, 2007). Several investigations have also dealt with dental materials (Keilig *et al.*, 2009) and dental/orthodontic implants (Gallas *et al.*, 2005). FEA has already been used in orthodontic research. Yettram *et al.* (1977) were among the first to employ a two-dimensional FE model of a maxillary central incisor to determine the centre of rotation during translational movements. Halazonetis (1996) used a similar two-dimensional model to determine PDL stress distribution following force application at varying distances from the centre of resistance of a maxillary incisor. Using more complex three-dimensional (3D) models, several investigators (Tanne *et al.*, 1987; McGuinness *et al.*, 1991; Wilson *et al.*, 1991) studied the moment-to-force ratios and stress distributions during orthodontic tooth movement. In the field of dentofacial orthopaedics, FE models have been employed to evaluate the stress distribution induced within the craniofacial complex during the application of orthopaedic chin cup forces (Tanne *et al.*, 1993) and conventional headgear forces (Tanne and Matsubara, 1996).

The FEA has also been applied to the evaluation of orthodontic attachments. Ghosh *et al.* (1995) have used 3D FE models of ceramic orthodontic bracket designs to

determine the stress distribution and cohesive failure within the bracket when a full dimension stainless steel arch wire is engaged within the bracket slot. Katona (1994) and Katona and Moore (1994) have used a two-dimensional FE model of the bracket tooth interface to assess the stress distribution in the system when bracket-removing forces are applied. Similarly, Rossouw and Terblanche (1995) have used a simplified 3D FE model to evaluate the stress distribution around orthodontic attachments during debonding. A study of Reimann *et al.* (2009) analysed the biomechanical behaviour of posterior teeth under headgear traction with neighbouring teeth in different eruption stages by using an FE model of the right part of a human maxilla. Bourauel *et al.* (2007) described in detail the application of FEMs in orthodontic biomechanics. In recent years, FE model analysis focused in the investigation of orthodontic mini-implants regarding their biomechanical performance and the stress distribution in the surrounding bone (Motoyoshi *et al.*, 2005; Motoyoshi *et al.*, 2009a,b; Stahl *et al.*, 2009).

The aim of this study was to examine the validity of the FE simulation when compared to experimental data, in an attempt to establish the reliability of the numerical (FE) method in relevant research, especially with respect to orthodontic mini-implants.

Material and methods

Experimental method

The purpose of the experimental part was to investigate the effect of implant length, implant diameter, and insertion mode on the primary stability of two different types of orthodontic mini-implants, by measuring their deflections during force application *in vitro*. The experiment is presented extensively in a previously publicized paper (Chatzigianni *et al.*, 2011), so it is only described briefly in this paper. Conical-shaped self-drilling titanium mini-implants with identical design from two different companies, Aarhus (American Orthodontics, Sheboygan, Wisconsin, USA) and LOMAS mini-screws (Mondeal, Mühlheim, Germany), were selected for this study. The animal bone consisted of fresh segments of bovine ribs with a clear defined cortical and cancellous bone. Each type of mini-implant was available in two different lengths (7 and 9 mm) and in a diameter of 1.5 mm. Additional LOMAS pins of 7 mm length were also available in a wide diameter of 2 mm. Mini-implants were inserted with two insertion modes, vertically to the bone surface or with an angulation of 45 degrees to the mesial direction, except for the 2 mm wide LOMAS pins which were only placed perpendicular to the bone surface. According to the above parameters, the original sample was divided into nine groups.

Following implant insertion, the specimens were fixed in a standard metallic cube using an autopolymerizing acrylic

resin (Palavit G, Heraeus Kulzer GmbH, Hanau, Germany). The preparations were then transferred and mounted in a 3D mobility measurement system (MOMS). The MOMS consists of two components, a mechanical part, for load application and a laser-optical subsystem, which registered the implant displacements and rotations in all three planes of space. An aluminium cube with three lased diodes is attached to the assembly. The laser beams of the cube were focused on planar positioning sensing detectors (PSD). The laser system was fixed on top of each mini-implant, thus defining a Cartesian rigid body coordinate system. A force of 0.5 N was applied on the neck of the mini-implants through closed nickel titanium (NiTi) coil springs (American Orthodontics). The force axis was parallel to the bone surface and to the horizontal along the mesio-distal direction. The force was applied twice to each specimen and mean value of the two readings was used for evaluation. Implant displacement and rotation were available in all three coordinates. The data collected were subsequently shown as force/deflection curves. This study focused on mini-implant displacements (D_x) along the direction of force (*x*-axis) and on mini-implant rotations (tipping movement) around the *y*-axis (R_y), which was vertical to the force direction.

Numerical method

Following measurements of force/deflection curves, one specimen of each group (nine in total) was randomly chosen and sent for scanning in a microCT (μCT) scanner to the University of Mainz (μCT40; SCANCO Medical AG, Brüttisellen, Switzerland). The number of slices in each scanned preparation ranged from 800 to 1035. Based on the sectional views of the μCT scans, a 3D surface reconstruction of the preparations including implant and bone was conducted using the custom-developed software ADOR-3D (Rahimi *et al.*, 2005). First of all, the boundaries of the structures (implant, cortical, and cancellous bone) were identified automatically and marked. Secondly, the boundaries were discretized and a 3D surface model was generated. Surface models were further processed to generate FE models. For this purpose, the surface models were imported into the FE package MSC.Marc/Mentat2007r1 (MSC Software Corp., Santa Ana, California, USA). Tetrahedral elements were used to mesh each model automatically.

The elements of each numerical model were divided into implant elements, cortical bone elements, and spongy bone elements. Critical part in this phase was the connection of mini-implant elements to bone elements and also the connection between cortical and spongy bone elements. For that, the tetrahedral meshing of bone elements was made in such way that bone elements became smaller and finer towards implant elements to improve the accuracy of the interfaces and the outcome of the numerical calculation.

Table 1 Number of elements of the FE models. Model 'H' was excluded.

Implant	Insertion	FE model	Element number		
			Implant	Cortical bone	Spongy bone
Aarhus 1.5 × 7 mm	Straight	A	43727	14630	51196
	Angled	B	39971	41198	33087
Aarhus 1.5 × 9 mm	Straight	C	34335	20840	68637
	Angled	D	35111	18445	70481
Lomas 1.5 × 7 mm	Straight	E	43832	27588	40495
	Angled	F	42306	27332	27978
Lomas 1.5 × 9 mm	Straight	G	50481	16954	69058
Lomas 2 × 7 mm	Straight	I	59128	23144	55215
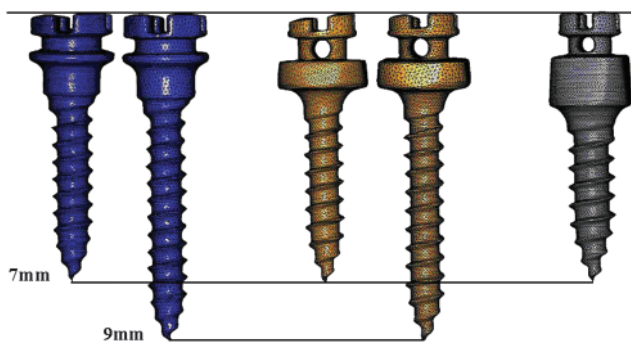
Figure 1 All five types of mini-implants as three-dimensional finite element models. Left to right: Aarhus 1.5 × 7 mm, Aarhus 1.5 × 9 mm, Lomas 1.5 × 7 mm, Lomas 1.5 × 9 mm, and Lomas 2 × 7 mm.

After tetrahedral meshing, which was done automatically by MSC.Marc/Mentat, the models were transferred into the program 3-matic (Materialise NV, Leuven, Belgium) for mesh refinement and manual element connection in those critical areas, where necessary. The number of tetrahedral elements used to mesh each model ranged from 110 000 to 130 000 (Table 1) and the number of nodes was around 16 000. As μCT scanning with the requested high resolution takes several hours and the specimens are heated during scanning, the samples would run dry during scanning. Consequently, specimens were sent to μCT scanning after experimentation.

In total, nine FE models of mini-implant and surrounding bone were generated (models A–I), representing the nine scanned experimental specimens. The generated FE mini-implant models, a typical μCT scan, and examples of the complete numerical models consisting of the mini-implant and surrounding bone are shown in Figures 1 and 2.

Concept of the combined experimental and numerical study

Once the 3D FE model was generated, the loading and boundary conditions and various parameters had to be adjusted in order to resemble as exactly as possible the experimental situation. This involved the direction and magnitude of force, the material and mechanical parameters of the model elements, and the contact parameters, such as frictional coefficient and contact forces.

Model loading and boundary conditions were adjusted to perfectly simulate the experimental tests, with the force applied along the mesio-distal direction up to a maximum of 0.5 N. Since the experimental mini-implant deflections were derived from the centre of the laser cube by the laser beam focusing on the detectors, an identical point was constructed for the registration of the numerical deflections. In order to further reproduce the experimental condition, the interface between the mini-implants and the bone was not fixed, in a way that friction between implant surface and bone bed was performed in so-called contact analyses to simulate the non-osseointegrated situation of the immediately loaded mini-implants. Furthermore, elements and nodes localized in the lower third part of the bone model were fixed in all three degrees of freedom in order to represent the bone part embedded in the acrylic resin during experimentation.

Both implant and bone elements (cortical and cancellous) were assumed to be homogenous, isotropic, and linearly elastic, which is an adequate approximation to this small deformation situation. Although this is not absolutely correct with respect to bone density and bone biomechanical behaviour, the influence of the bone on the pin deflections is standardized and the individual pin characteristics become more clearly. Previous sensitivity analyses have shown that geometrical differences (thickness of cortical bone, pin length, pin diameter, and implant bed) have higher impact on the reaction of the system than bone quality, we assume that a variation of spongious bone Young's modulus would have only minor influence on the simulated pin reaction (Stahl *et al.*, 2009). The material properties of implant, cortical, and cancellous bone elements were characterized of a Young's modulus of 110, 10, and 0.3 GPa, respectively, and with a Poisson's ratio (ν) set to 0.3.

Statistical analysis

Numerical results were compared to the experimental ones using the Altman–Bland test (Bland and Altman 1996).
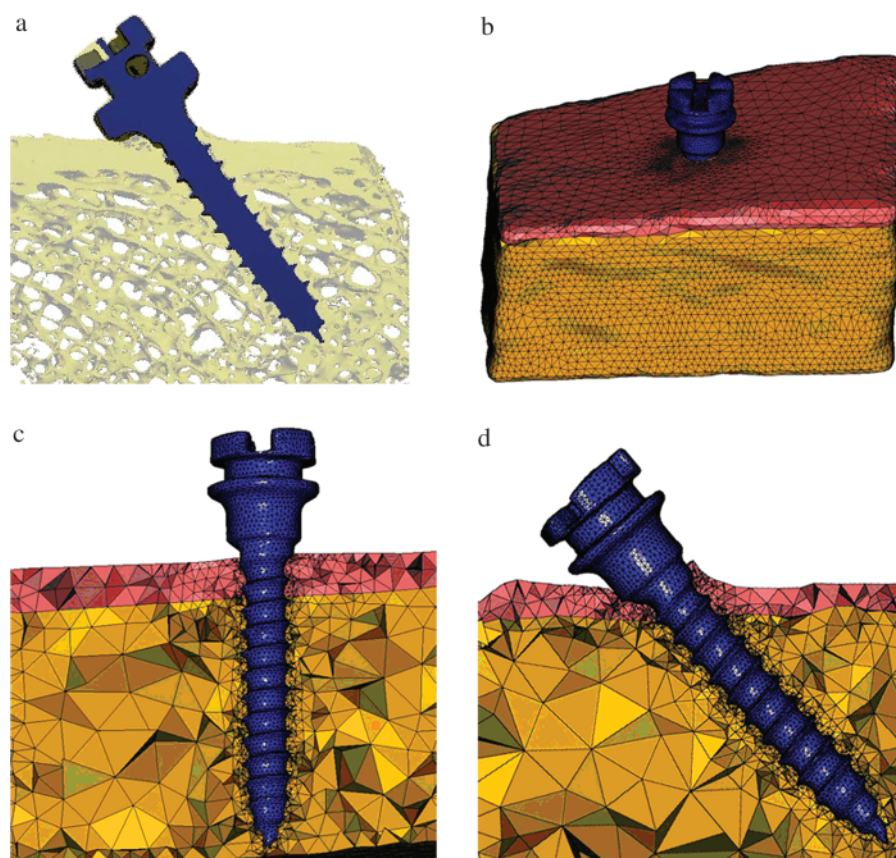
Figure 2 Example of three-dimensional (3D) view of a microCT (µCT)-scanned specimen (a). Example of a 3D finite element model of mini-implant (Aarhus 1.5 × 9 mm) and surrounding bone in full view (b) after reconstructed from µCT scans; same model in cutting planes of straight (c) and of 45 degree of insertion (d).

Differences were further presented by using difference plots and a graphical technique called Youden plot. Statistical analysis has been performed with STATA (StataCorp LP, College Station, Texas, USA) software for the Altman–Bland test and with MedCalc Software (MedCalc Software, Mariakerke, Belgium) for the Youden plot.

Results

Experimental results

The results of the experimental part of this study were previously analysed (Chatzigianni *et al.*, 2011) and had shown that at low force levels (0.5 N), no statistically significant difference in mini-implant displacement according to implant length and implant diameter was observed. Mini-implant insertion angle also did not influence its stability (Chatzigianni, 2010). Rotation of mini-implants (tipping movement) was only influenced by implant type, with LOMAS mini-implants tending to rotate more than the Aarhus mini-implants.

Comparison between experimental and FEA

One theoretical (FE) model of the nine reconstructed did not work properly in the simulation due to numerical instabilities and was excluded from further analysis (model H). On the eight remaining models, the numerical values of mini-implant displacement and rotation, registered on the 0.5 N force level, were compared to the corresponding experimental values.

Intra-observer agreement between experimental and numerical values did not show statistically significant differences for displacement measurements and marginally not significant (NS) for rotation measurements (P = NS, Table 2). The *in vitro* displacement of mini-implants measured in micrometre could be more accurately reproduced by the computer than their rotation. Each mini-implant deflection values registered in the experiment and in the simulation are shown in Table 3 and Figure 3. A schematic representation is further shown with difference plots (Figure 4).

A more detailed analysis using the Youden plot showed quite good coincidence between experimental and numerical

values (Figure 5). For this plot, a horizontal median line was drawn parallel to the *x*-axis so that there should be as many points above the line as there were below it. A second median line was drawn parallel to the *y*-axis so that there should be as many points on the left as there were on the right of this line. Outliers are not used in determining the position of the median lines. The intersection of the two median lines is termed the Manhattan median. The circle drawn should include 95 per cent of the experimental

observations, if the individual constant errors could be eliminated. A 45 degree reference line was drawn through the Manhattan median so that observations far from the line and outside of the circle indicated a systematic and random error. Collectively, the experimental and numerical outcomes showed a good agreement, especially regarding mini-implant displacement.
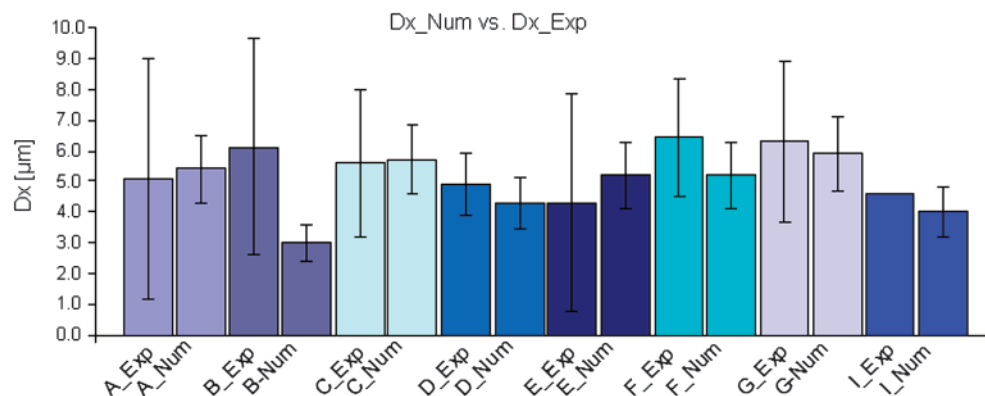
Stress and strain distributions

In this study, the maximum von Mises stress and strain distributions in the bone elements surrounding each mini-implant after 0.5 N force application were calculated. In all numerical models, stress in the cortical bone was concentrated at the bone margin in the direction of force and the maximum value registered was 4.4 MPa. Total strains in the cancellous bone concentrated along the surface of the mini-implant opposite to the direction of force application and its maximum value were 1195 μstrain, with those maximum values concentrated at the thread peaks (Table 4).

Table 2 Altman–Bland test between experimental and numerical results for mini-implant displacement (Dx) and rotation (Ry).

Altman–Bland test	For Dx (μm)	For Ry (°)
n	8	8
95% CI for differences	−1.58–0.43	−0.0002–0.0104
t statistic	−1.35	2.29
Degrees of freedom	7	7
P	0.22 not significant 95% limits of agreement	0.06 marginally not significant 95% limits of agreement
Lower	−2.94	−0.0073
Upper	1.79	0.0175

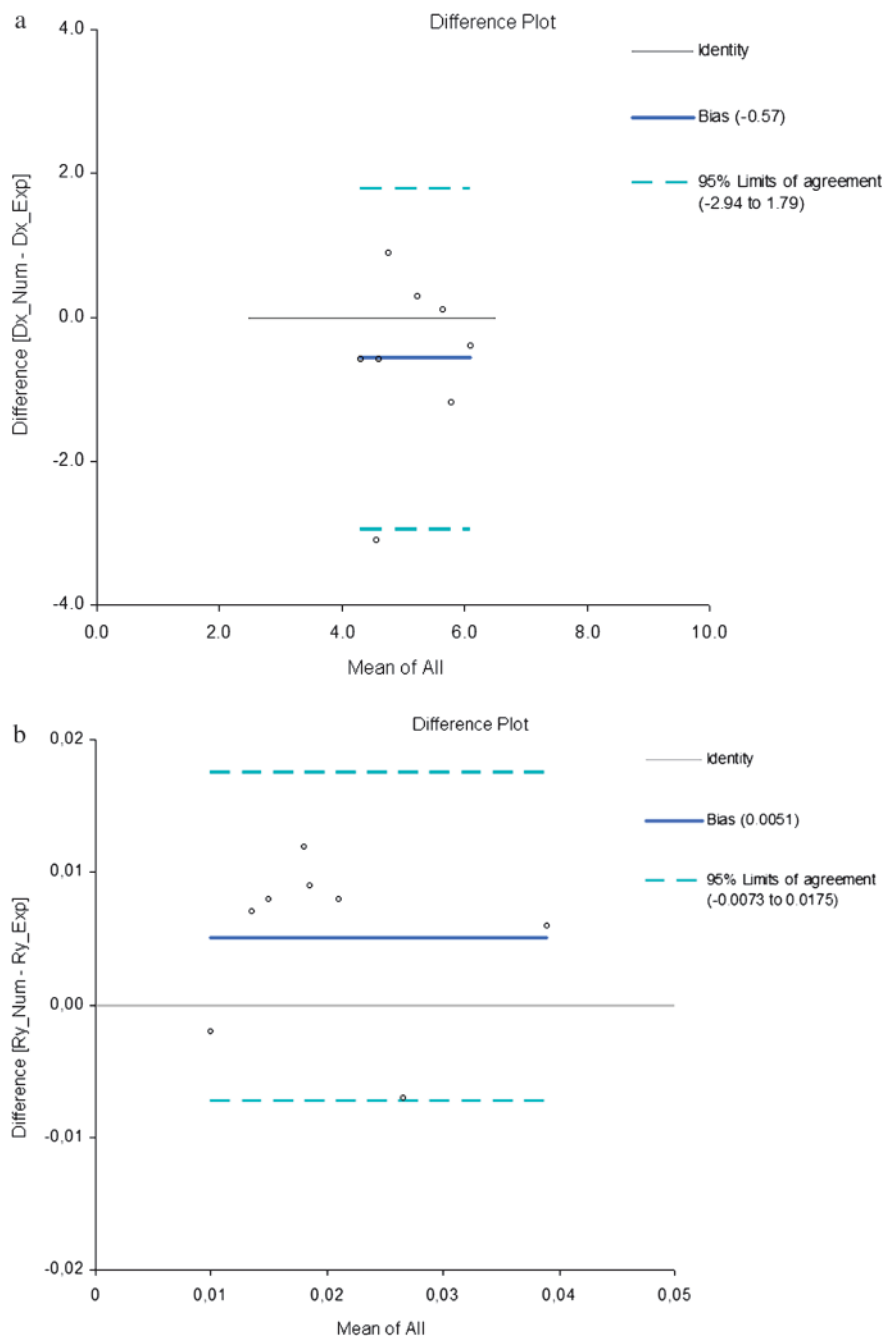**Discussion**

In the present study, both FE mini-implant and bone models were accurately reconstructed from the original *in vitro* models by μCT scanning and the purpose was to compare the numerical and experimental results, which showed a good agreement. In this study, it was both experimentally and numerically evidenced that when a small force level of 0.5 N is applied, no difference in mini-implant primary stability, as represented by its displacement, according to implant length, implant diameter, and insertion mode is present. Nevertheless, impact of mini-implant dimensions on their stability has been controversial among investigators.

Apart from implant dimensions, bone remodelling around a mini-implant can affect its stability. In the field of implantology, the stress and strain generated in the cortical and cancellous bone during loading are of great importance since the stimulated remodelling processes in the peri-implant area may be critical for mini-implant

Table 3 Experimental and numerical displacement (Dx) and rotation (Ry) values at the force level of 0.5 N.

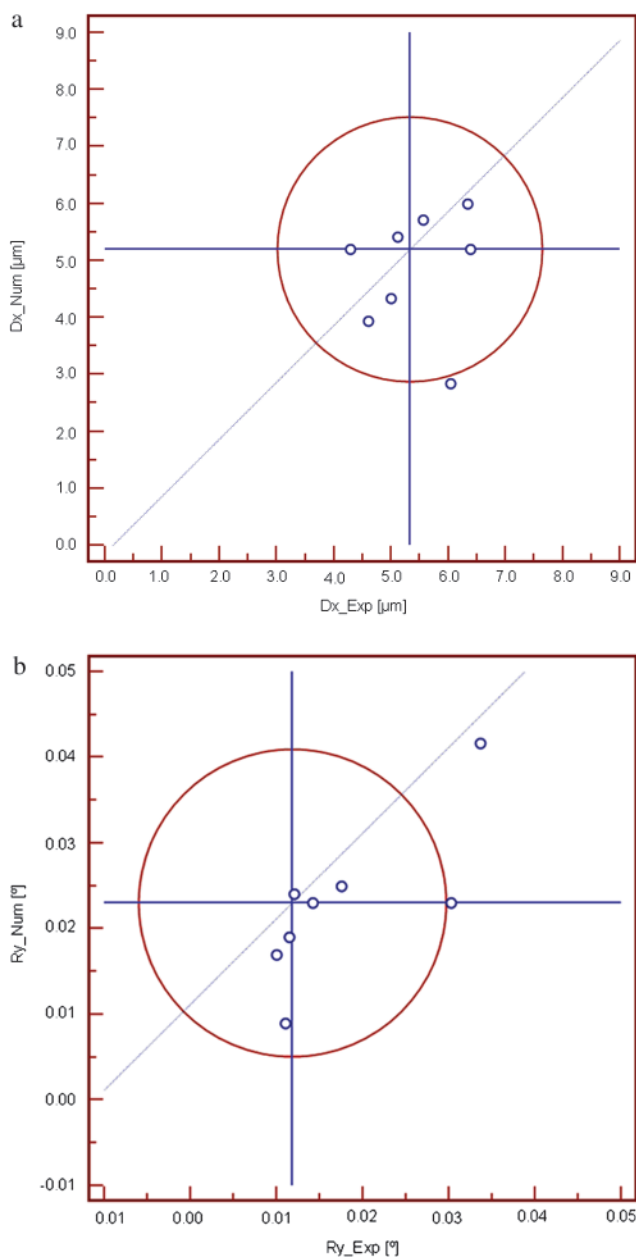| Models		Dx_Exp (μm)	Dx_Num (μm)	Ry_Exp (°)	Ry_Num (°)
Aarhus	A	5.1	5.4	0.030	0.023
	B	6.1	3.0	0.011	0.009
	C	5.6	5.7	0.036	0.042
	D	4.9	4.3	0.011	0.019
LOMAS	E	4.3	5.2	0.017	0.025
	F	6.4	5.2	0.014	0.023
	G	6.3	5.9	0.012	0.024
	I	4.6	4.0	0.010	0.017

Figure 3 Diagram of experimental and numerical values of the models.

Figure 4 Difference plots for displacement Dx (a) and rotation Ry (b) between experimental and numerical values.

survival. The FEA is a method converting complex implant-to-bone interactions into theoretical designs. The amount and direction of force and the cortical bone thickness are some of the factors affecting the stress generated during traction. In this study, maximum stress and strain values after low force application, with the force axis parallel to the bone surface and with a cortical bone thickness around 2 mm, were in general within the physiological limits.

It is important to note that the numerical FE models used in this study were not constructed but reconstructed from original experimental preparations. For that reason, this study did not compare the data generated here to other investigations and did not extensively analyse stress and strain distribution. Our study showed that the numerical results were a confirmation to our experimental data. It seems that the FE method is developing to a useful and reliable tool for many sciences with many applications in the field of dentistry and orthodontics.

Table 4 Maximum stress and strain values of cortical and spongy bone at low force level.

Model	Stress (MPa) cortical	Strain (µstrain) spongy
A	3.4	669
B	1.4	370
C	3.1	1,195
D	3.0	806
E	3.5	435
F	4.2	495
G	4.4	940
I	2.5	565

3D surface model and 3D FE model generation, problems can occur due to improper visualization, improper method, and improper parameter installation, i.e. identification of structures in the slices, number of slices, smoothing factor, material and mechanical parameters, as well as boundary conditions, which may cause model distortion. The result of these may be the loss of information leading to poor quality of the reconstruction of the original structure or to a non-functional model. As noted previously, in this study, one of nine numerical models, named model 'H' and representing the LOMAS 1.5×9 mm mini-implant, did not work properly in the simulation due to unknown reason and was excluded from further analysis.

Nevertheless, software packages offering the possibility of FEA undergo constant improvement. More complex tooth models and model assumptions are being developed by sophisticated computer programs. Nowadays, FEA is a very promising tool in dentistry and in orthodontics to understand a number of tissue properties and biomechanical problems.

Concluding, the FEA of this study provided theoretical evidence about mini-implant stability as measured by their deflection. In particular, the FEA results seemed to correlate well with corresponding *in vitro* data, both showing that at low force levels, no influence of mini-implant dimensions and insertion angle on mini-implant primary stability could be observed. Our results suggest that when the applied force magnitude is low, as during tooth intrusion or indirect anchorage, mini-implants with small dimensions can be safely used. This study revealed a tendency that the FEA offers a promising alternative to experimental procedures.

Figure 5 Youden plot. More detailed comparison between experimental and numerical values. (a) Displacement Dx_Exp to Dx_Num and (b) Rotation Rx_Exp to Rx_Num.

Apart from the benefits of the FEA, the limitations of the method should be considered. Starting from the first numerical models generated which were quite simple, it was understood that the value of FEA entirely depends on element density and the accuracy of geometry, material properties, and loading conditions of the examined structure. The more complex the model under investigation the more difficult the FEA is. Problems can occur at every step during 3D model generation starting even from the µCT scanning. Improper position in the scan or improper scanning parameters can lead to model defects. At next stages, during

References

Bland J M, Altman D G 1999 Measuring agreement in method comparison studies. Statistical Methods in Medical Research 8: 135–160

Bourauel C, Keilig L, Rahimi A, Reimann S, Ziegler A, Jäger A 2007 Computer-aided analysis of the biomechanics of tooth movements. International Journal of Computational Dentistry 10: 25–40

Chatzigianni A 2010 Experimental and numerical analysis of the biomechanical characteristics of orthodontic mini-implants. University of Bonn, Bonn

Chatzigianni A, Keilig L, Reimann S, Eliades T, Bourauel C 2011 Effect of mini-implant length and diameter on primary stability under loading with two force levels. European Journal of Orthodontics 33: 381–387

Farah J W, Craig R G, Sikarskie D L 1973 Photoelastic and finite element stress analysis of a restored axisymmetric first molar. Journal of Biomechanics 6: 511–520

Gallas M M, Abeleira M T, Fernández J R, Burguera M 2005 Three-dimensional numerical simulation of dental implants as orthodontic anchorage. European Journal of Orthodontics 27: 12–16

Ghosh J, Nanda R S, Duncanson M G Jr, Currier G F 1995 Ceramic bracket design: an analysis using the finite element method. American Journal of Orthodontics and Dentofacial Orthopedics 108: 575–582

Halazonetis D J 1996 Computer experiments using a two-dimensional model of tooth support. American Journal of Orthodontics and Dentofacial Orthopedics 109: 598–606

Katona T R 1994 The effects of load location and misalignment on shear/peel testing of direct bonded orthodontic brackets-a finite element model. American Journal of Orthodontics and Dentofacial Orthopedics 106: 395–402

Katona T R, Moore B K 1994 The effects of load misalignment on tensile load testing of direct bonded orthodontic brackets—a finite element model. American Journal of Orthodontics and Dentofacial Orthopedics 105: 543–551

Kawarizadeh A, Bourauel C, Jäger A 2003 Experimental and numerical determination of initial tooth mobility and material properties of the periodontal ligament in rat molar specimens. European Journal of Orthodontics 25: 569–578

Keilig L, Stark H, Bayer S, Utz K H, Strazza M, Grüner M, Bourauel C 2009 Numerical investigation of the mechanical loading of supporting soft tissue for partial dentures. International Journal of Prosthodontics 22: 201–203

Knox J, Jones M L, Hubsch P, Middleton J, Kralj B 2000 An evaluation of the stresses generated in a bonded orthodontic attachment by three different load cases using the Finite Element Method of stress analysis. Journal of Orthodontics 27: 39–46

McGuinness N J, Wilson A N, Jones M L, Middleton J 1991 A stress analysis of the periodontal ligament under various orthodontic loadings. European Journal of Orthodontics 13: 231–242

Motoyoshi M, Inaba M, Ono A, Ueno S, Shimizu N 2009a The effect of cortical bone thickness on the stability of orthodontic mini-implants and on the stress distribution in surrounding bone. International Journal of Oral and Maxillofacial Surgery 38: 13–18

Motoyoshi M, Ueno S, Okazaki K, Shimizu N 2009b Bone stress for a mini-implant close to the roots of adjacent teeth-3D finite element analysis. International Journal of Oral and Maxillofacial Surgery 38: 363–368

Motoyoshi M, Yano S, Tsuruoka T, Shimizu N 2005 Biomechanical effect of abutment on stability of orthodontic mini-implant. A finite element analysis. Clinical Oral Implants Research 16: 480–485

Natali A N, Carniel E L, Pavan P G, Bourauel C, Ziegler A, Keilig L 2007 Experimental-numerical analysis of minipig's multi-rooted teeth. Journal of Biomechanics 40: 1701–1708

Rahimi A *et al.* 2005 3D reconstruction of dental specimens from 2D histological images and microCT-scans. Computer Methods in Biomechanics and Biomedical Engineering 8: 167–176

Reimann S *et al.* 2009 Numerical and clinical study of the biomechanical behaviour of teeth under orthodontic loading using a headgear appliance. Medical Engineering and Physics 31: 539–546

Rossouw P E, Terblanche E 1995 Use of finite element analysis in assessing stress distribution during debonding. Journal of Clinical Orthodontics 29: 713–717

Stahl E, Keilig L, Abdelgader I, Jäger A, Bourauel C 2009 Numerical analyses of biomechanical behavior of various orthodontic anchorage implants. Journal of Orofacial Orthopedics 70: 115–127

Tanne K, Matsubara S 1996 Association between the direction of orthopedic headgear force and sutural responses in the nasomaxillary complex. Angle Orthodontist 66: 125–130

Tanne K, Matsubara S, Sakuda M 1993 Stress distributions in the maxillary complex from orthopedic headgear forces. Angle Orthodontist 63: 111–118

Tanne K, Sakuda M, Burstone C J 1987 Three-dimensional finite element analysis for stress in the periodontal tissue by orthodontic forces. American Journal of Orthodontics and Dentofacial Orthopedics 92: 499–505

Yettram A L, Wright K W J, Houston W J B 1977 Centre of rotation of a maxillary central inscisor under orthodontic loading. British Journal of Orthodontics 4: 23–27

Wilson A N, Middleton J, McGuinness N, Jones M 1991 A finite element study of canine retraction with a palatal spring. British Journal of Orthodontics 18: 211–218